A Cuticle Collagen Encoded by the *lon-3* Gene May Be a Target of TGF-β Signaling in Determining *Caenorhabditis elegans* Body Shape

Yo Suzuki, Gail A. Morris, Min Han and William B. Wood[1]

Department of Molecular, Cellular and Developmental Biology, University of Colorado, Boulder, Colorado 80309-0347

Manuscript received July 30, 2002
Accepted for publication September 6, 2002

ABSTRACT

The signaling pathway initiated by the TGF-β family member DBL-1 in *Caenorhabditis elegans* controls body shape in a dose-dependent manner. Loss-of-function (*lf*) mutations in the *dbl-1* gene cause a short, small body (Sma phenotype), whereas overexpression of *dbl-1* causes a long body (Lon phenotype). To understand the cellular mechanisms underlying these phenotypes, we have isolated suppressors of the Sma phenotype resulting from a *dbl-1(lf)* mutation. Two of these suppressors are mutations in the *lon-3* gene, of which four additional alleles are known. We show that *lon-3* encodes a collagen that is a component of the *C. elegans* cuticle. Genetic and reporter-gene expression analyses suggest that *lon-3* is involved in determination of body shape and is post-transcriptionally regulated by the *dbl-1* pathway. These results support the possibility that TGF-β signaling controls *C. elegans* body shape by regulating cuticle composition.

HOW do animals dictate the correct proportional sizes for their body parts? Although factors such as growth hormone are known to play pivotal roles, genetic regulation of body size and body shape is still poorly understood (reviewed in Conlon and Raff 1999). Recent findings in Drosophila suggest that factors involved in size regulation, for example, insulin-like growth factor signaling, are conserved among metazoans (reviewed in Edgar 1999), validating the utility of studying model organisms for better understanding of this process.

In *Caenorhabditis elegans*, a TGF-β signaling pathway has been implicated in regulation of body size and body shape. Loss-of-function (*lf*) mutations in the *dbl-1* gene, which encodes the TGF-β family ligand DBL-1, or in genes encoding the receptors and Smad transcription factors of the *dbl-1* pathway cause a Sma phenotype (reviewed in Patterson and Padgett 2000). Conversely, hyperactivation of this pathway (*e.g.*, by means of *dbl-1* overexpression) causes a Lon phenotype (Morita *et al.* 1999; Suzuki *et al.* 1999). Mutations in three genes, *lon-1*, *lon-2*, and *lon-3*, cause a similar Lon phenotype (Brenner 1974), suggesting that these genes have related functions in body morphology regulation. However, the cellular mechanisms controlled by the *dbl-1* pathway are largely unknown.

Other mutations that cause changes in body shape are those in the *dpy* and *sqt* genes, many of which have been shown to encode cuticle collagens (*e.g.*, Kramer *et al.* 1988; von Mende *et al.* 1988). These mutations cause shorter body length, and a few alleles and allelic combinations result in Lon phenotypes (Kusch and Edgar 1986; reviewed in Kramer 1994). Dpy and Sqt mutant animals appear short and fat but generally no thinner than wild type, in contrast to Sma animals, which are also short but more normally proportioned. Whether Dpy and Sqt cuticle defects are related to changes in activity of the *dbl-1* pathway was previously unclear.

Here we present evidence suggesting that *dbl-1* regulation of body shape may be partly accomplished by a cellular mechanism that involves regulation of cuticle composition. To identify possible regulatory targets of the *dbl-1* pathway, we screened for suppressors of the Sma phenotype caused by a *dbl-1* mutation and found two that are alleles of the *lon-3* gene. We show that *lon-3* encodes a collagen that is a component of the *C. elegans* cuticle and that it may be regulated post-transcriptionally by the *dbl-1* pathway.

MATERIALS AND METHODS

***C. elegans* strains:** All strains were cultured using standard methods (Brenner 1974). The alleles used in these experiments (all in the N2 wild-type background) were as follows, in map order by linkage group (LG). Unless otherwise noted, the references for these alleles are found in Riddle *et al.* (1997). LGI: *cye-1(ku256)* (Fay and Han 2000), *unc-13(e450)*; LGII: *sma-6(wk7)* (Krishna *et al.* 1999), *dpy-2(e8)* and *(e1359)*, *sqt-1(sc103)* and *(sc101)*; LGIII: *lon-1(e185)*, *sma-4(e729)*, *unc-119(ed3)*; LGIV: *dpy-9(e12)*, *him-8(e1489)*; LGV: *unc-46(e177)*, *dbl-1(ev580)* and *(wk70)* (Suzuki *et al.* 1999), *dbl-1(nk3)* (obtained from Morita *et al.* 1999), *ctDf1*, *sma-1(e30)*, *vab-8(e1017)*, *sqt-3(sc63ts)*, *lon-3(e2175)*, *lon-3(sp5)*, *(sp6)*, and *(sp23)* (obtained from A. Leroi, personal communication), *lin-25(e1446)*, *him-5(e1467)*, *unc-76(e911)*; LGX: *dpy-7(e88)*, *lon-2(e678)*. The small deficiency *ctDf1* uncovers *sma-1*, *vab-8*, and *sqt-3* (Manser and Wood 1990). Except as noted above, all alleles were obtained from the Caenorhabditis Genetics Cen-

Sequence data from this article have been deposited with the EMBL/GenBank Data Libraries under accession no. AF465981.

[1]*Corresponding author:* 347 UCB, Boulder, CO 80309-0347.
E-mail: wood@stripe.colorado.edu

ter or from our collection. The *dbl-1* overexpression array *kuEx136* was generated by injecting a *dbl-1* genomic clone, pYS1 (Suzuki *et al.* 1999), at 100 ng/μl with no other markers and picking Lon progeny. The transmission frequency of this array was ~100%.

Suppressor screens and complementation tests: *dbl-1(ev580)* animals (Sma) were mutagenized with EMS using a standard protocol (Brenner 1974). On the basis of the number of F_1 progeny, we screened an estimated 14,000 haploid genomes. Suppressed animals, either non-Sma or Lon, were isolated in the F_2 generation.

Suppressed animals were crossed with N2 males to generate males heterozygous for the new mutations as well as *dbl-1 (ev580)*; these heterozygotes were crossed with *lon-1(e185)* or *lon-3(e2175)* homozygous hermaphrodites. The presence of Lon male progeny indicated noncomplementation. Some of the suppressed animals, upon crossing with N2 males, produced Lon males but no Lon hermaphrodites, indicating that these mutants contain recessive, *X*-linked *lon* mutations.

Phenotypic and genetic analysis of *lon-3* mutants: Unless indicated otherwise, body size phenotypes were analyzed only by direct observation using a dissecting microscope. Measurements of body length were performed using Scale Master II (Calculated Industries) on Nomarski images captured and printed using Scion Image (Scion, Frederick, MD).

To test if *lon-3* mutations are dominant or recessive, N2 males were crossed with *lon-3(e2175)* hermaphrodites, and these animals were transferred daily; the second plate contained 173 wild-type (WT) males, 180 WT hermaphrodites, and 10 Lon hermaphrodites (presumably self-progeny). WT hermaphrodites from this cross were indistinguishable when compared side by side with N2 wild-type hermaphrodites of similar stages. Similar crosses of N2 males to other *lon-3* mutants (hermaphrodite) also produced WT progeny, except one mutant, *ct418*, which produced only semi-Lon (cross) and Lon (self) progeny. These results indicate that *e2175*, *ct417*, *sp5*, *sp6*, and *sp23* are recessive and that *ct418* is semidominant.

RNAi experiments were performed as described (Fire *et al.* 1998). A T7 polymerase promoter was attached to both ends of the exon 1 sequence using PCR with primers CMo42 and CMo442 (C. Mello, personal communication) and with the template pYSL3C1 (see below). Double-stranded (ds) RNA was prepared using the MEGAscript T7 kit (Ambion, Austin, TX). In addition to the Lon phenotype, *lon-3(RNAi)* resulted in a low level (~5%) of late embryonic arrest. We did not carefully characterize this possibly nonspecific effect. The effectiveness of *lon-3* RNAi was demonstrated when injection of *lon-3* dsRNA abolished the green fluorescent protein (GFP) expression from the translational fusion construct pYSL3G3 (see below), as well as the Rol phenotype caused by the same construct, and caused a Lon phenotype in injected animals.

Cloning of *lon-3*: Cosmids, C27A7, ZK863, and ZK836, and subclones, pYSL3S1 and pYSL3S2 (see below), were injected at 20 ng/μl into the *lon-3(e2175)* mutant with 100 ng/μl of pTG96 (a GFP reporter plasmid; Yochem *et al.* 1998). pYSL3S2 contained only one predicted intact open reading frame (WormBase; http://www.wormbase.org).

The initiator methionine predicted in WormBase appears to be the *bona fide* initiator on the basis of our finding that five sequenced 5′-RACE products terminated at 24, 35, 36 (two independent PCR products), and 37 bp before the predicted initiator methionine. The exon-intron structure was determined using PCR of reverse transcribed samples.

The *lon-3* cDNA sequence has been submitted to GenBank (accession no. AF465981).

Plasmid construction: An 11-kb *Pst*I-*Sal*I fragment from the cosmid ZK863 was cloned into pBluescript II SK+ (Stratagene, La Jolla, CA) to generate pYSL3S1. A 5.5-kb *Bam*HI-*Xho*I fragment from pYSL3S1 was cloned into pBluescript II SK+ to generate pYSL3S2. This construct contains 2.5 kb of the 5′ sequence, the complete coding sequence including the sole intron, and 2 kb of the 3′ sequence. A 2.5-kb *Bam*HI-*Hae*III fragment from pYSL3S2 containing ~2.5 kb of the *lon-3* 5′ sequence and the first five codons of the *lon-3* coding sequence was cloned into the *Bam*HI and *Sma*I sites of the GFP vector pPD95.67 (A. Fire, personal communication) to generate the "transcriptional" reporter gene pYSL3G1. The "translational" reporter gene pYSL3G3 had the complete 5′ and coding sequences present in pYSL3S2, followed by a GFP sequence, the last eight codons repeated of the *lon-3* coding sequence, the native *lon-3* stop codon, and the complete 3′ sequence of pYSL3S2. To generate this plasmid, PCR with primer sequences, TGGTGGGC-GGCGCC (*Nar*I)-GTAAGCACAAGA GAGTCTAC (the end of the *lon-3* coding sequence)-ATGAG TAAAGGAGAAGAACTTTTCAC (the beginning of the GFP sequence) and TGGTGGGC-GGCGCC (*Nar*I)-GATCCCCCG GGCATTTGTATAG (the end of the GFP sequence), was used to generate a fragment that had the GFP sequence connected to the last part, from the *Nar*I site to the end, of the *lon-3* coding sequence. This fragment flanked by *Nar*I sites was cloned into the unique *Nar*I site of pYSL3S2. For RNAi experiments, an 840-bp PCR fragment flanked by *Bam*HI sites, containing only the complete exon one sequence, was cloned into pBluescript II SK+ to generate pYSL3C1. The portions of these plasmids amplified by PCR were sequenced to confirm that no errors were introduced by PCR.

Lesions of *lon-3* alleles: PCR fragments amplified from genomic DNA samples isolated from *lon-3* mutants were directly sequenced. Lysis of animals was performed for 2 hr at 60° in 10 mm Tris-HCl (pH 8.3), 50 mm KCl, 2.5 mm $MgCl_2$, 0.45% Tween-20, 0.05% gelatin, and 500 μg/ml proteinase K. Sequencing of the coding region revealed the lesions of *sp6* (R^{114} [CGA] → stop [TGA]), *sp23* (W^{36} [TGG] → stop [TAG]), *ct417* (W^{36} [TGG] → stop [TAG]), and *ct418* (G^{61} [GGA] → E [GAA]). The lesion for *sp5* was not found in this region. For *e2175*, which contained a gross aberration to the *lon-3* sequence, a PCR fragment that spanned the lesion was identified and sequenced. *e2175* lacked part of the *lon-3* sequence (−2001 bp to +388 bp in relation to the initiator ATG codon) and contained part of the transposon Tc5 (1 bp to 2779 bp; see Collins and Anderson 1994) in a left-to-right orientation.

Expression of *lon-3*: For reporter expression analyses, pYSL-3G1 and pYSL3G3 were injected at 100 and 20 ng/μl, respectively, to *unc-119; him-5* animals with 30 ng/μl of pDP#MM 016B (an *unc-119* rescuing plasmid; Maduro and Pilgrim 1995). Some of these *lon-3::gfp* arrays were integrated using 3000 R of gamma irradiation, followed by six backcrosses with *unc-119; him-5* and N2. The *lon-3::gfp* expression patterns did not change before and after integration. The integrated arrays *kuIs56* (pYSL3G1) and *kuIs55* (pYSL3G3) were used to assess the effects of various mutations on *lon-3* expression.

Probably due to the punctate nature of the *lon-3* translational reporter-gene expression patterns, we were unable to analyze the pixel intensity of its digitized photographs. To compare the intensity of expression in different mutant backgrounds, we instead relied on "by eye" scoring. Unless otherwise noted, individual L4 animals with the identical Christmas-tree vulval structure were mounted on a slide and photographed with shortest exposure possible to UV to minimize photobleaching of GFP. These photographs were given unlabeled (blind scoring) to a scorer to be evaluated by eye and rated for fluorescence intensity on a scale of one to six (in the case of the translational construct) or of one to five (in the case of the transcriptional construct), where one represents the lowest intensity.

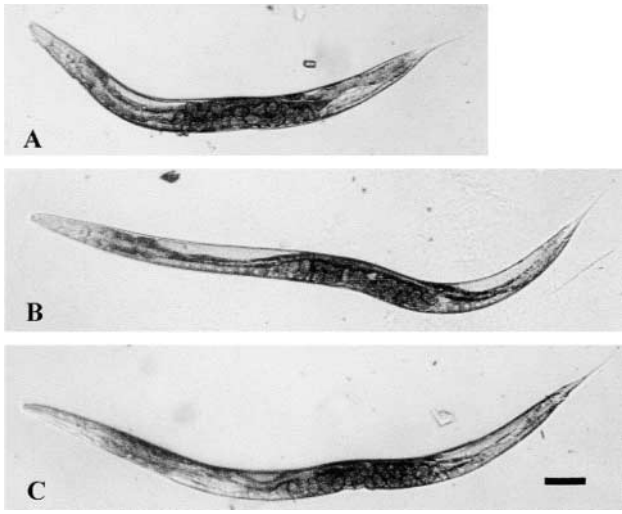

FIGURE 1.—Lon phenotypes resulting from a *lon-3* mutation and from *dbl-1* overexpression. (A) N2 wild-type hermaphrodite. (B) *lon-3(ct417)* mutant hermaphrodite. (C) Hermaphrodite overexpressing *dbl-1* from *kuEx136* (see MATERIALS AND METHODS). These photographs show adult animals grown for 52 hr posthatching at ~25°. Bar, 0.1 mm.

For the *lon-3* transcriptional reporter gene (pYSL3G1), additional methods were used. Progeny from *dbl-1(ev580)* heterozygotes that carried an integrated array of this construct were scored for body size and fluorescence intensity under a dissecting microscope equipped with UV epi-illumination. Although some variation in fluorescence was observed in these animals, there was no correlation between the fluorescence intensity and the Sma or WT body size phenotypes of these animals. Furthermore, when WT and Sma progeny were compared quantitatively using Scion Image, no significant difference in brightness was detected (data not shown).

RESULTS

Suppressors of the Sma phenotype caused by a *dbl-1(lf)* mutation define *lon-3*: To understand the mechanisms downstream of *dbl-1* signaling in body shape regulation, we screened 14,000 haploid genomes for suppressors of the Sma phenotype caused by a *dbl-1* mutation (see MATERIALS AND METHODS). We isolated 14 mutations, of which 2 that produced Lon phenotypes were alleles of *lon-1* and have been reported previously (MORITA *et al.* 2002; see also MADUZIA *et al.* 2002). The remaining mutations, which produced non-Sma phenotypes, included two alleles of *lon-3*, which were designated *ct417* and *ct418* (see MATERIALS AND METHODS). In addition to these new *lon-3* alleles and the reference allele *e2175* (BRENNER 1974) used for complementation tests, three other alleles, *sp5*, *sp6*, and *sp23*, have been found in the *lon-3* gene (A. LEROI, personal communication).

***lon-3* is required for body length restriction:** All *lon-3* alleles, when homozygous, caused Lon phenotypes similar to each other and to the Lon phenotype of *dbl-1* overexpressing animals (Figure 1; the adult column in Table 1). In *lon-3* animals Lon phenotypes were not seen in early larval stages but became evident by the adult stage (Table 1). In contrast, *dbl-1* overexpressing animals were Lon in the L3 stage as well as in the adult stage (Table 1).

TABLE 1

Comparison of body lengths in *lon-3* mutant and *dbl-1* overexpressing animals

	Body length (mm)		
Strain	L1	L3	Adult
Wild type (N2)	0.25 ± 0.02	0.51 ± 0.05	1.11 ± 0.08
lon-3(ct417)	0.24 ± 0.02	0.50 ± 0.04	1.35 ± 0.06
dbl-1 overexpression (*kuEx136*)	0.24 ± 0.02	0.66 ± 0.04	1.37 ± 0.06

Starved L1 animals were fed for 0, 24, and 48 hr at ~25° to generate L1, L3, and adult animals, respectively. Length measurements are shown as mean values ±SD.

The *lon-3(ct418)* mutation was semidominant, whereas other alleles were apparently recessive (see MATERIALS AND METHODS). RNAi of *lon-3* causes the same Lon phenotype in wild-type animals and does not enhance the Lon phenotype in a *lon-3* mutant (Table 2), suggesting that the Lon phenotype is the null body shape phenotype of *lon-3*. No additional phenotypes such as embryonic lethality or male tail phenotypes were observed in *lon-3* homozygotes or hemizygotes (data not shown).

***lon-3* mutations are only partially epistatic to *dbl-1* pathway mutations:** Since *lon-3* alleles were isolated as suppressors of the Sma phenotype caused by a *dbl-1* mutation, *lon-3* may function downstream of or in parallel to the *dbl-1* pathway. However, animals carrying null mutations for *dbl-1* (*nk3*; MORITA *et al.* 1999) and *lon-3* (*ct417*; see below for molecular lesion) had an intermediate phenotype (Table 2). One possible interpretation of this result is that *lon-3* mediates only a subset of *dbl-1* functions.

***lon-3* encodes a *C. elegans* cuticle collagen:** *lon-3* was previously mapped to LGV (BRENNER 1974) and shown to be uncovered by chromosomal deletions *ctDf1* (MANSER and WOOD 1990) and *arDf1* (see SUNDARAM and GREENWALD 1993). Using a series of three-factor mapping crosses with genetic markers uncovered by these deletions (Table 3), we mapped *lon-3* to a small region between *sma-1* and *vab-8* (Figure 2). The Lon phenotype of *e2175* could be rescued by either of two overlapping cosmids (ZK863 and ZK836) in this region and by subclones containing the overlapping sequence. The only intact predicted open reading frame (ZK836.1) in the smaller of these subclones, pYSL3S2, encodes a protein with characteristics of *C. elegans* cuticle collagens. On the basis of the positions of cysteines (reviewed in KRAMER 1997), the predicted LON-3 protein belongs to the SQT-1 subgroup. The exon-intron structure was determined

TABLE 2

Body lengths of animals defective in *lon-3*, *dbl-1*, or both

Strain	Body length (mm)		
	L1	L3	Adult
Wild type (N2)	0.25 ± 0.02	0.63 ± 0.02	1.30 ± 0.03
lon-3(ct417)	0.24 ± 0.02	0.65 ± 0.02	1.50 ± 0.05
dbl-1(nk3)	0.25 ± 0.02	0.50 ± 0.03	0.65 ± 0.06
dbl-1 lon-3[a]	0.25 ± 0.01	0.49 ± 0.05	0.85 ± 0.03
lon-3(RNAi)[b]	ND	ND	1.50 ± 0.04
lon-3(ct417RNAi)[c]	ND	ND	1.49 ± 0.04
lon-3(ct417RNAi)[c]	ND	ND	1.49 ± 0.06
lon-3(ct417RNAi)[c]	ND	ND	1.48 ± 0.04

Starved L1 animals were fed for 0, 24, and 48 hr at ~25° to generate L1, L3, and adult animals, respectively. Length measurements are shown as mean values ±SD. ND, not done.

[a] Similarly, intermediate length phenotypes were observed in all of the following double mutants: *lon-3(e2175)* and *sma-4(e729)*, *sma-6(wk7)*, or *dbl-1(ev580)*; *lon-3(ct417)* and *dbl-1(ev580)*; and *lon-3(ct418)* and *dbl-1(ev580)* (data not shown).

[b] *lon-3* dsRNA (see MATERIALS AND METHODS) was injected into N2 wild-type hermaphrodites. *lon-3(RNAi)* produced Lon animals from six out of seven dsRNA-injected animals (86%). Body lengths were measured on the progeny of one injected animal.

[c] *lon-3* dsRNA was injected into hermaphrodites carrying the indicated *lon-3* mutant allele. Body lengths were measured on the progeny of three individual dsRNA-injected animals.

using PCR of reverse transcribed samples. We did not detect a splice leader, SL1 or SL2, using 5′-RACE (see MATERIALS AND METHODS) or RT-PCR with SL-specific primers (data not shown), suggesting that the *lon-3* transcript is not transspliced. [While this article was in revision, similar results on cloning and identification of *lon-3* were reported (NYSTROM *et al.* 2002).]

Molecular lesions were found in five out of six *lon-3* alleles, indicating that *lon-3* encodes this collagen protein (Figure 3; see MATERIALS AND METHODS). *sp6*, *sp23*, and *ct417* are nonsense mutations upstream of the sequence encoding the Gly-X-Y domain, which is expected to generate the collagen triple helix. Therefore, these alleles are likely to be severe loss-of-function or null mutations. Since *ct418* is semidominant, the G-to-E substitution it is predicted to cause may create a dominant negative form of LON-3. The reference allele *e2175* lacks 2.4 kb of the *lon-3* sequence and has an insertion of part of the transposon Tc5. No lesion in the coding sequence was found for *sp5*, suggesting that this mutation could be in a *lon-3* regulatory sequence.

Reporter-gene analysis suggests that *lon-3* encodes a cuticle component: We determined the expression of an integrated reporter gene that contained the entire 2.5-kb 5′ sequence present in the rescuing clone pYSL3S2 and the first five amino acids including the initiator methionine connected to the GFP sequence with an SV40 nuclear localization signal (the transcriptional reporter gene pYSL3G1; see MATERIALS AND METHODS). GFP fluorescence was localized in the nuclei of most, if not all, hypodermal cells (Figure 4A). Expression was first detected in the pretzel stage just prior to hatching. The GFP signal gradually intensified toward the young adult stage and then diminished.

To test experimentally the possibility that *lon-3* encodes a cuticle component, we examined the expression

TABLE 3

Three-factor mapping of *lon-3*

Genotype of heterozygote			Phenotype of recombinants	Recombinants with *lon-3* / total recombinants
lon-3	+	+	Vab non-Lin	0/4
+	*vab-8*	*lin-25*		
lon-3	+	+	Lin non-Vab	13/13
+	*vab-8*	*lin-25*		
lon-3	+	+	Vab non-Sqt	0/2
+	*vab-8*	*sqt-3*		
lon-3	+	+	Sqt non-Vab	2/2
+	*vab-8*	*sqt-3*		
+	*lon-3*	+	Vab non-Sma	2/8
sma-1	+	*vab-8*		
+	*lon-3*	+	Sma non-Vab	6/6
sma-1	+	*vab-8*		

Alleles used for marker genes are listed in MATERIALS AND METHODS.

patterns of another reporter gene that contained the entire coding sequence, in addition to the 5′ and 3′ sequences present in pYSL3S2 (the translational reporter gene pYSL3G3; see MATERIALS AND METHODS). GFP fluorescence was faint, but clearly observable on the surface of the larval and adult animal, presumably in the cuticle (Figure 4B). This reporter gene did not rescue the Lon phenotype of *lon-3* mutants, but instead caused an adult Rol (*Rol*ler) phenotype both in *lon-3* mutants and in N2 wild type. These results suggest the cuticular localization of the reporter-gene product.

***lon-3* appears to be post-transcriptionally regulated by the *dbl-1* pathway:** To test the possibility that *dbl-1* affects *lon-3* expression, we examined the GFP expression from the *lon-3* translational reporter gene (pYSL3G3) in various mutant backgrounds. When we placed the integrated array (*kuIs55*) containing this reporter gene in *dbl-1* mutant backgrounds, the GFP expression appeared to be increased (Figure 4, C and D). To more quantitatively assess the effects of *dbl-1* and other pathway genes on the GFP expression, we rated the GFP expression intensities by eye using blind scoring (see MATERIALS AND METHODS). In these experiments, the GFP expression was upregulated in *dbl-1* and *sma-4* mutants and was downregulated in *dbl-1* overexpressing animals (Table 4; Figure 4, E–G). The Rol phenotypes of these mutant animals were indistinguishable under the dissecting microscope. These animals apparently lacked alae in the adult stage, so that we could not use these structures to count the number of twists of the body. This upregulation of reporter expression in *dbl-1* and *sma-4* mutants is not likely to result from a higher concentration of the GFP signal simply due to the small body size of *dbl-1* mutants, since mutations such as *dpy-2(e8)*, *dpy-7(e88)* (Table 4), *unc-46(e177)*, and *dpy-9(e12)* (data not shown), which also cause smaller body size, did not affect GFP expression from pYSL3G3.

In contrast, when we compared GFP expression from the *lon-3* transcriptional reporter gene (pYSL3G1) in wild-type and *dbl-1(lf)* backgrounds, we observed no differences in the intensity of GFP expression, suggesting that *lon-3* transcription is not affected by the *dbl-1* pathway (Table 5; see MATERIALS AND METHODS). These results suggest that the *dbl-1* pathway regulates *lon-3* expression post-transcriptionally, presumably by modulating processing of *lon-3* mRNA, degradation of *lon-3* mRNA or the LON-3 protein, or synthesis of the LON-3 protein.

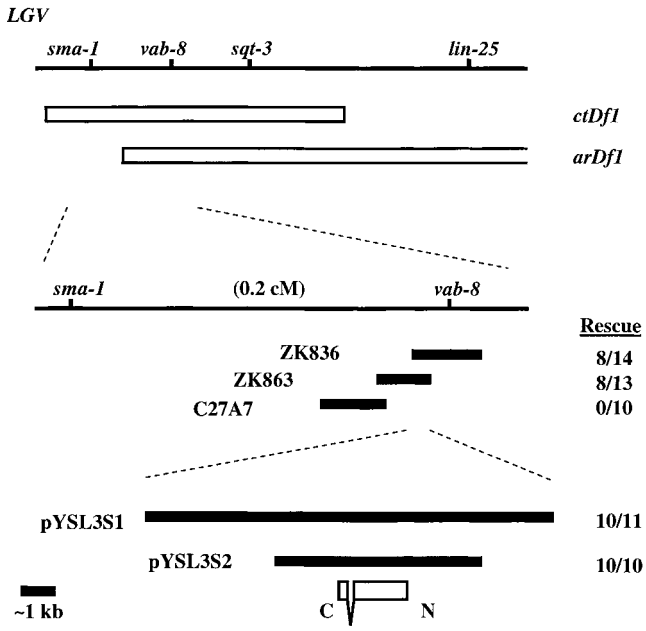

FIGURE 2.—Cloning of *lon-3*. Genetic and physical maps of the *lon-3* region are shown (see text). pYSL3S1 and pYSL3S2 are subclones of ZK863 (see MATERIALS AND METHODS). Presumably due to the overexpression of *lon-3*, some rescued animals were shorter than wild type.

***lon-3* GFP expression is affected by *dbl-1* pathway and some cuticle-related mutations, but not by mutations that cause altered ploidy:** To understand the relationship between *lon-3* and other *lon* genes, we placed the *lon-3* translational reporter gene in various *lon* mutation backgrounds. A *lon-2* mutation downregulated the GFP expression, whereas a *lon-1* mutation or the Lon allele (*sc101*) of *sqt-1* (KRAMER and JOHNSON 1993) had no effect (Table 4). This result is interesting because *lon-2* is

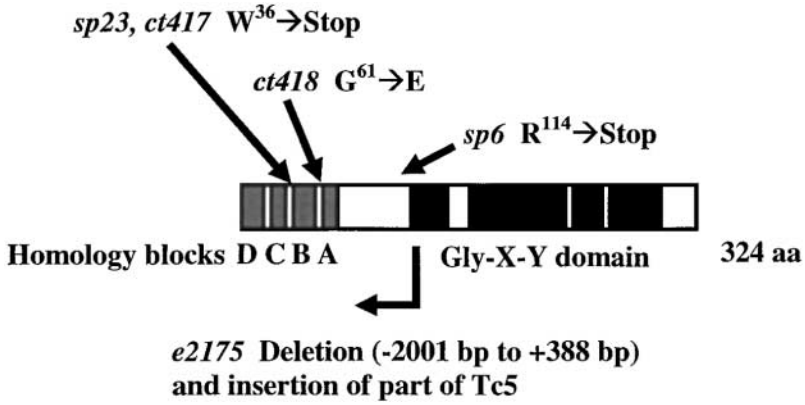

FIGURE 3.—Structure of the predicted LON-3 protein. Homology blocks (see text) are shown in gray (KRAMER 1997). The Gly-X-Y domain with a few gaps (white) is shown in black. Molecular lesions corresponding to five *lon-3* alleles are indicated by arrows (see MATERIALS AND METHODS). The *lon-3* cDNA sequence is found in GenBank (accession no. AF465981).

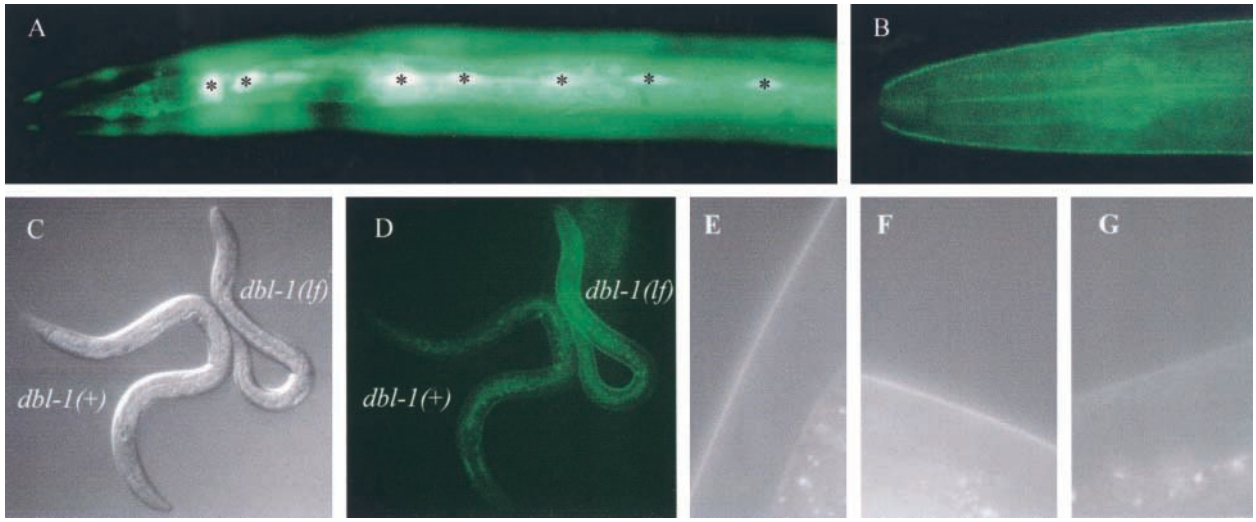

Figure 4.—Expression patterns of *lon-3::gfp* reporter transgenes. Integrated lines carrying *lon-3::gfp* reporter genes were generated as described in materials and methods. (A) L4 hermaphrodite carrying a transcriptional reporter gene with an SV40 nuclear localization signal (pYSL3G1) as an integrated array (*kuIs56*). GFP is localized to the nuclei of hypodermal cells; many are out of focus. Asterisks indicate nuclei of lateral hypodermal cells (seam cells). (B) Head region of an adult hermaphrodite carrying a translational fusion construct (pYSL3G3) as an integrated array (*kuIs55*). Note the GFP expression outlining the animal. (C–G) Comparison of GFP expression levels from *kuIs55* in *dbl-1(+)*, *dbl-1(lf)*, and *dbl-1* overexpression (*kuEx136*) genetic backgrounds. These animals are at precisely the same stage based on vulval morphology. C and D show *dbl-1(+)* and *dbl-1(wk70)* animals. In D, the contrast was adjusted to visualize the low level of GFP expression in the *dbl-1(+)* animal. E–G are three of the photographs used to generate Table 4, showing animals with close to the average rating of GFP expression among the *dbl-1(+)*, *dbl-1(nk3)*, and *kuEx136* groups, respectively. The same exposure setting was used for all the images in E–G with no contrast adjustment. Light spots in E–G are caused by autofluorescence of gut granules and are unrelated to *lon-3* expression.

thought to function upstream of *dbl-1* (Y. Suzuki and W. B. Wood, unpublished observations; S. Baird, C. Savage-Dunn and R. Padgett, personal communication). From this result, *lon-1* and *sqt-1* appear to be unrelated or to function downstream of or in parallel to *lon-3*. *lon-1* is a dose-dependent regulator of adult hypodermal ploidy (Morita *et al.* 2002). To see if ploidy change has any effect on *lon-3* expression, we used a cyclin E mutation that is known to reduce hypodermal ploidy at least in older adults (A. Flemming, A. Leroi and D. Fay, personal communication). We did not see any difference in *lon-3* expression in adults of a *cye-1*; *unc-13* strain relative to adults of the *unc-13* control (Table 4).

To uncover possible interactions among collagens in the cuticle, we placed the *lon-3* translational reporter gene in *sqt-1*, *dpy-2*, and *dpy-7* mutation backgrounds. The null allele (*sc103*) of *sqt-1* (Kramer and Johnson 1993) slightly enhanced the GFP expression although the Lon allele (*sc101*) of *sqt-1* appeared to have no effect (Table 4). Allele specificity was also observed with *dpy-2*, where the *e8* allele had no effect, while the *e1359* allele caused a dramatic reduction in GFP expression. *dpy-2(e8)* and *dpy-7(e88)* cause substitutions for Gly in the Gly-X-Y domain (Johnstone *et al.* 1992; Levy *et al.* 1993), whereas the lesion of *dpy-2(e1359)* is not known. The alteration of GFP expression by collagen mutations supports the hypothesis that *lon-3* product is present in the cuticle.

DISCUSSION

Cuticle modeling may be a target of the TGF-β (*dbl-1*) pathway in *C. elegans* body shape control: We have identified mutations in *lon-3* as suppressors of the Sma phenotype caused by a *dbl-1* mutation and shown that *lon-3* encodes a *C. elegans* cuticle-type collagen. On the basis of our studies of its expression patterns, *lon-3* appears to be a cuticle component. GFP from the *lon-3* transcriptional fusion construct is observed in most if not all hypodermal nuclei, and GFP from the *lon-3* translational fusion construct is observed on the surface of the animals, presumably in the cuticle. The translational construct contains additional sequences not present in the transcriptional construct, such as the sole intron and the 3′ sequence. These sequences may have caused differences in transcription of the two reporters and could account for our observation that expression from the transcriptional construct is more robust than that from the translational construct. Results obtained with the translational reporter must be interpreted with care because it does not rescue the Lon phenotype of *lon-3* mutants, despite including all the sequences that are present in the rescuing clone.

With this caveat, changes of *lon-3* reporter-gene expression patterns in *dbl-1* mutants seen with the translational construct, but not with the transcriptional construct, suggest that either processing or degradation of the *lon-3* mRNA, or synthesis, processing, or degradation

TABLE 4

The intensity of GFP expression from a translational fusion construct

Genotype	GFP expression intensity[a]	No. of animals examined
Wild type (N2)	3.5 ± 1.1	40
Body shape mutations		
dbl-1(nk3)	4.1 ± 1.1 ($P < 0.001$)[b]	25
sma-4(e729)	4.2 ± 0.9 ($P < 0.005$)	25
dbl-1 overexpression (*kuEx136*)	3.0 ± 1.1 ($P < 0.05$)	40
lon-1(e185)	3.3 ± 0.8 ($P = 0.7$)	25
lon-2(e678)	2.7 ± 0.9 ($P < 0.005$)	40
Other collagen mutations		
sqt-1(sc103)	3.9 ± 0.8 ($P < 0.05$)	25
sqt-1(sc101)	3.4 ± 1.3 ($P = 0.5$)	25
dpy-2(e8)	3.1 ± 1.1 ($P = 0.7$)	25
dpy-2(e1359)	2.1 ± 1.0 ($P < 0.005$)	25
dpy-7(e88)	3.4 ± 1.0 ($P = 0.5$)	25
Ploidy mutations		
unc-13(e450)[c]	2.4 ± 0.9	25
cye-1(ku256) unc-13(e450)[c]	2.7 ± 0.7 ($P = 0.09$)	25

[a] The intensity of GFP expression in individual animals (L4 stage unless indicated otherwise) was rated one to six (six highest), using blind scoring (see MATERIALS AND METHODS). Averages are shown ±SD. Student's *t*-test was used to calculate *P* values.

[b] Significance values refer only to the pairwise comparisons of each mutant mean to the wild type and not to comparisons between mutant means. Data from the first 25 out of the total 40 N2 animals were used to calculate the *P* values for animals with the sample size of 25.

[c] Adult animals (which have lower *lon-3::gfp* expression than L4 animals) were used for these experiments. These animals were obtained by incubating the eggs laid within a 1-hr period for 72 hr at 20°. In all other experiments, L4 animals displaying a characteristic Christmas-tree vulval structure were used.

of the LON-3 protein, is regulated by the *dbl-1* pathway. This regulation of *lon-3* by the *dbl-1* pathway may be direct or indirect. We have found that *lon-3* expression is affected in an allele-specific manner by *sqt-1* and *dpy-2*. It has been shown recently that *lon-3* mutations interact genetically with *sqt-1* and *rol-6* (NYSTROM *et al.* 2002). It is equally plausible that these collagen genes are the direct targets of the *dbl-1* pathway and encode binding partners of the LON-3 protein, affecting the stability or incorporation of the LON-3 protein in the cuticle. Body shape phenotypes (*e.g.*, Dpy phenotype) caused by mutations in previously known cuticle component genes appear to be slightly different from the Sma phenotype caused by *dbl-1* pathway mutations (see Introduction). Our results provide the first evidence of a link between the cuticle and the *dbl-1* pathway.

To further evaluate whether *lon-3* represents a true downstream target gene, the mechanism responsible for its regulation (*e.g.*, protein degradation, translational control, and mRNA processing) must be clarified. A microarray study has found that a predicted collagenase gene is downregulated in a *dbl-1* mutant, suggesting the possibility that LON-3 is controlled by the *dbl-1* pathway through this collagenase (MOCHII *et al.* 1999). Our preliminary observations indicate, however, that silencing of this collagenase gene using RNAi does not cause a Sma phenotype or an increase in reporter expression from the *lon-3* translational fusion construct (Y. SUZUKI and W. B. WOOD, unpublished results). Because some collagens encoded by the *dpy* genes are presumably involved in functions opposite to those of *lon-3*, the regulation of collagen turnover may be complex. Testing the effects of inactivating other metalloproteinase genes and characterization of other suppressors isolated in our genetic screen may help to elucidate the mechanisms of *lon-3* regulation.

Arguments for a branched *dbl-1* pathway with multiple regulatory targets: Earlier studies have shown that the *dbl-1* pathway is involved in the control of body shape and cell size (MORITA *et al.* 1999; SUZUKI *et al.* 1999), as well as the ploidy of normally polyploid hypodermal cells (FLEMMING *et al.* 2000), but the relationships between these effects have been unclear. Mutations in *dbl-1* pathway genes cause a reduction in body size and hypodermal nuclear ploidy in adults (FLEMMING *et al.* 2000), whereas mutations in the *lon-1* gene cause an increase in body length and ploidy (MORITA *et al.* 2002). However, it is unclear whether the effect of these mutations is primary or secondary. For example, it is possible that cuticle defects or other structural changes resulting from these mutations affect cell size, and cell size only secondarily affects ploidy. Consistent with this possibility

TABLE 5

Intensity of GFP expression from a transcriptional fusion construct

Genotype	GFP expression intensity	No. of animals examined
Wild type	2.4 ± 1.1	25
dbl-1(nk3)	2.4 ± 0.8 ($P = 0.9$)	25

The intensity of GFP expression in individual animals was rated one to five (five highest), using blind scoring (see MATERIALS AND METHODS). L4 animals displaying a characteristic Christmas-tree vulval structure were used. No significant difference in intensity was observed between wild type and *dbl-1(nk3)*.

are the findings that *dbl-1* overexpression does not appear to cause increase in ploidy (NYSTROM *et al.* 2002) and that only a subset of *lon-1* alleles affects ploidy, although all cause Lon phenotypes (MORITA *et al.* 2002). MORITA *et al.* (2002) have presented evidence that *lon-1* is regulated by the *dbl-1* pathway.

Our results together with the above findings suggest a branched pathway in which *lon-3* functions downstream of the *dbl-1* pathway as one of perhaps several independent targets of *dbl-1* signaling (Figure 5). Another of these targets may be *lon-1*. This model is based on the following arguments:

1. *lon-3* expression is affected in opposite ways by *dbl-1(lf)* mutations and *dbl-1* overexpression, suggesting that *lon-3* does not act by an independent pathway to determine body shape. A *lon-2* mutation, like *dbl-1* overexpression, decreases *lon-3* expression (Table 4), consistent with *lon-2* acting as an upstream regulator of the *dbl-1* pathway.
2. However, double mutants carrying both *lon-3* and *dbl-1* mutations are neither Lon nor Sma, but exhibit an intermediate phenotype, suggesting that *lon-3* acts in only one branch of the *dbl-1* pathway.
3. Branching is likely to occur downstream of Smads because both *dbl-1* and *sma-4*, which encodes the common Smad transcription factor of the Smad complexes, affect *lon-3* expression patterns similarly (Table 4).
4. Effects of various mutations on *lon-3* expression and ploidy, which may be controlled by *lon-1*, appear to be independent events, suggesting independent branches of the pathway. Mutations in *lon-3* affect body shape but not ploidy (NYSTROM *et al.* 2002), and mutations that cause changes in ploidy do not appear to affect *lon-3* expression (Table 4). Mutations in *lon-1* affect body shape but do not appear to affect *lon-3* expression (Table 4). Finally, the effects of *lon-1* and *lon-3* mutations on body size are additive: *lon-1*; *lon-3* double mutants are longer than either of the single mutants (NYSTROM *et al.* 2002). Thus independent downstream branches could include one for *lon-3*-mediated control of cuticle composition and another for *lon-1*-mediated control of ploidy (Figure 5).

A third branch, mediated by unknown proteins, would be consistent with the finding that *dbl-1* pathway mutations affect body size from the L2 stage onward, while *lon-3* effects are seen only in adults (Tables 1 and 2). This branch may employ *lon-1* or perhaps additional collagen genes controlled by the *dbl-1* pathway (Figure 5). The collagen genes we and others (NYSTROM *et al.* 2002) have shown to interact with *lon-3* are candidates for such genes. If they are controlled at the level of transcription, microarray analysis may be a fruitful approach to identifying them among the ~150 predicted *C. elegans* collagen genes (reviewed in JOHNSTONE 2000).

Extracellular matrix and growth: Various collagen genes are targets of TGF-β regulation in mammals (reviewed in MASSAGUE 1990), although the mammalian role of TGF-β is to activate collagen expression and not to repress it as in the case of *lon-3* regulation by *dbl-1*. At least for *lon-3* (other collagen genes have not been tested), *dbl-1* does not appear to affect transcription, which is unlike the mechanism of mammalian collagen regulation by TGF-β; hence these interactions may not be conserved.

In mammals, production of collagens signifies a differentiated state for cells, when growth is inhibited. The importance of collagen remodeling for tissue growth has been demonstrated by mice mutated for a matrix metalloproteinase gene. These mice exhibit dwarfism among other tissue remodeling defects (HOLMBECK *et al.* 1999). The situation appears to be similar in *C. elegans*, where LON-3 collagen production imposes restrictions on body elongation. Therefore, *C. elegans* may be a promising model system for studying mechanisms of growth and remodeling of extracellular matrix, as well as relationships between them.

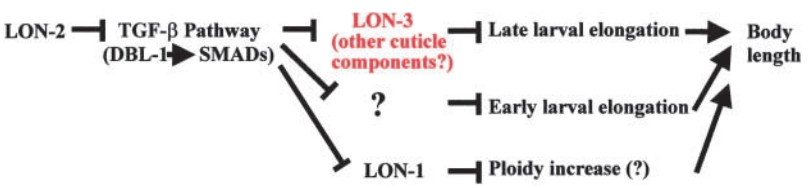

FIGURE 5.—A model for regulation of body size control by the *dbl-1* pathway. LON-3 may represent a branch pathway specific to late larval elongation. This regulation is likely to be post-transcriptional. LON-1 controls ploidy of adult hypodermal nuclei and is also a candidate target of the *dbl-1* pathway. Additional unknown targets may mediate early larval elongation, which the *dbl-1* pathway also appears to control.

We thank A. Leroi for *lon-3* alleles (*sp5*, *sp6*, and *sp23*), A. Fire for GFP vectors, The Caenorhabditis Genetics Center for *C. elegans* mutant strains, F. Wang and A. Keith for technical assistance, and members of the Boulder/Denver *C. elegans* community for helpful discussions. This work was supported by National Institutes of Health grant HD-14958 to W.B.W.

LITERATURE CITED

Brenner, S., 1974 The genetics of *Caenorhabditis elegans*. Genetics **77:** 71–94.

Collins, J. J., and P. Anderson, 1994 The Tc5 family of transposable elements in *Caenorhabditis elegans*. Genetics **137:** 771–781.

Conlon, I., and M. Raff, 1999 Size control in animal development. Cell **96:** 235–244.

Edgar, B. A., 1999 From small flies come big discoveries about size control. Nat. Cell Biol. **1:** E191–E193.

Fay, D. S., and M. Han, 2000 Mutations in *cye-1*, a *Caenorhabditis elegans* cyclin E homolog, reveal coordination between cell-cycle control and vulval development. Development **127:** 4049–4060.

Fire, A., S. Xu, M. K. Montgomery, S. A. Kostas, S. E. Driver *et al.*, 1998 Potent and specific genetic interference by double-stranded RNA in *Caenorhabditis elegans*. Nature **391:** 806–811.

Flemming, A. J., Z. Z. Shen, A. Cunha, S. W. Emmons and A. M. Leroi, 2000 Somatic polyploidization and cellular proliferation drive body size evolution in nematodes. Proc. Natl. Acad. Sci. USA **97:** 5285–5290.

Holmbeck, K., P. Bianco, J. Caterina, S. Yamada, M. Kromer *et al.*, 1999 MT1-MMP-deficient mice develop dwarfism, osteopenia, arthritis, and connective tissue disease due to inadequate collagen turnover. Cell **99:** 81–92.

Johnstone, I. L., 2000 Cuticle collagen genes. Expression in *Caenorhabditis elegans*. Trends Genet. **16:** 21–27.

Johnstone, I. L., Y. Shafi and J. D. Barry, 1992 Molecular analysis of mutations in the *Caenorhabditis elegans* collagen gene *dpy-7*. EMBO J. **11:** 3857–3863.

Kramer, J. M., 1994 Genetic analysis of extracellular matrix in *C. elegans*. Annu. Rev. Genet. **28:** 95–116.

Kramer, J. M., 1997 Extracellular matrix, pp. 471–500 in *C. elegans II*, edited by D. L. Riddle, T. Blumenthal, B. Meyer and J. R. Priess. Cold Spring Harbor Laboratory Press, Cold Spring Harbor, NY.

Kramer, J. M., and J. J. Johnson, 1993 Analysis of mutations in the *sqt-1* and *rol-6* collagen genes of *Caenorhabditis elegans*. Genetics **135:** 1035–1045.

Kramer, J. M., J. J. Johnson, R. S. Edgar, C. Basch and S. Roberts, 1988 The *sqt-1* gene of *C. elegans* encodes a collagen critical for organismal morphogenesis. Cell **55:** 555–565.

Krishna, S., L. L. Maduzia and R. W. Padgett, 1999 Specificity of TGFbeta signaling is conferred by distinct type I receptors and their associated SMAD proteins in *Caenorhabditis elegans*. Development **126:** 251–260.

Kusch, M., and R. Edgar, 1986 Genetic studies of unusual loci that affect body shape of the nematode *Caenorhabditis elegans* and may code for cuticle structural proteins. Genetics **113:** 621–639.

Levy, A. D., J. Yang and J. M. Kramer, 1993 Molecular and genetic analysis of the *Caenorhabditis elegans dpy-2* and *dpy-10* collagen genes: a variety of molecular alterations affect organismal morphology. Mol. Biol. Cell **4:** 803–817.

Maduro, M., and D. Pilgrim, 1995 Identification and cloning of *unc-119*, a gene expressed in the *Caenorhabditis elegans* nervous system. Genetics **141:** 977–988.

Maduzia, L. L., T. L. Gumienny, C. M. Zimmerman, H. Wang, P. Shetgiri *et al.*, 2002 *lon-1* regulates *Caenorhabditis elegans* body size downstream of the *dbl-1* TGFbeta signaling pathway. Dev. Biol. **246:** 418–428.

Manser, J., and W. Wood, 1990 Mutations affecting embryonic cell migrations in *Caenorhabditis elegans*. Dev. Genet. **11:** 49–64.

Massague, J., 1990 The transforming growth factor-beta family. Annu. Rev. Cell Biol. **6:** 597–641.

Mochii, M., S. Yoshida, K. Morita, Y. Kohara and N. Ueno, 1999 Identification of transforming growth factor-beta-regulated genes in *Caenorhabditis elegans* by differential hybridization of arrayed cDNAs. Proc. Natl. Acad. Sci. USA **96:** 15020–15025.

Morita, K., K. L. Chow and N. Ueno, 1999 Regulation of body length and male tail ray pattern formation of *C. elegans* by a member of TGF-beta family. Development **126:** 1337–1347.

Morita, K., A. J. Flemming, Y. Sugihara, M. Mochii, Y. Suzuki *et al.*, 2002 A *Caenorhabditis elegans* TGF-beta, DBL-1, controls the expression of LON-1, a PR-related protein, that regulates polyploidization and body length. EMBO J. **21:** 1063–1073.

Nystrom, J., Z. Z. Shen, M. Aili, A. J. Flemming, A. Leroi *et al.*, 2002 Increased or decreased levels of *Caenorhabditis elegans lon-3*, a gene encoding a collagen, cause reciprocal changes in body length. Genetics **161:** 83–97.

Patterson, G. I., and R. W. Padgett, 2000 TGF beta-related pathways. Roles in *Caenorhabditis elegans* development. Trends Genet. **16:** 27–33.

Riddle, D. L., T. Blumenthal, B. J. Meyer and J. R. Priess (Editors), 1997 *C. elegans II*. Cold Spring Harbor Laboratory Press, Cold Spring Harbor, NY.

Sundaram, M., and I. Greenwald, 1993 Suppressors of a *lin-12* hypomorph define genes that interact with both *lin-12* and *glp-1* in *Caenorhabditis elegans*. Genetics **135:** 765–783.

Suzuki, Y., M. D. Yandell, P. J. Roy, S. Krishna, C. Savage-Dunn *et al.*, 1999 A BMP homolog acts as a dose-dependent regulator of body size and male tail patterning in *Caenorhabditis elegans*. Development **126:** 241–250.

von Mende, N., D. Bird, P. Albert and D. Riddle, 1988 *dpy-13*: a nematode collagen gene that affects body shape. Cell **55:** 567–576.

Yochem, J., T. Gu and M. Han, 1998 A new marker for mosaic analysis in *Caenorhabditis elegans* indicates a fusion between hyp6 and hyp7, two major components of the hypodermis. Genetics **149:** 1323–1334.

Communicating editor: B. J. Meyer